

PREPARATION AND STUDY OF Cr₂O₃ ELECTROCOATINGS*

C. Gheorghies, L. Gheorghies

University "Dunarea de Jos" of Galati, Dept. of Physics, Str. Domneasca, No. 47, Romania

Graphite support was electrolytically coated with Cr₂O₃ from a 0.1 M aqueous solution of chromium nitrate hydrate with ethanol additives. On substrate material polycrystalline Cr₂O₃ was formed at current densities from 3 to 35 mA/cm² and deposition time of 5 to 30 min. The coating weight increased with current density and deposition time. Microstructural investigation shows that sintering of the Cr₂O₃ coatings at 1100°C for 1 hour in reducing atmosphere causes the densification of the coating. Structural characterisation of the electrodeposited coatings, by X-ray diffraction method and optical microscopy has been performed. The role of the (OH)⁻ groups during electrodeposition process by NMR method was carrying out. Generation of the (OH)⁻ groups and their migration in the solution lead to a change of the solution pH. The sintering process in a reducing atmosphere enhanced the densification of the coatings by reducing of the partial pressure as reported elsewhere. The densification process occurs by filling the microcracks between the islands with condensed chromia droplets. The electrodeposition process occurs in three distinct stages. In the first stage, on the cathode the germs of a porous layer appear, then the coating becomes relative homogeneous and, finally, ruggedness appears.

(Received August 3, 2000; accepted February 9, 2001)

Keywords: Electrodeposition, Chromia, X-ray diffraction

1. Introduction

The preparation of ceramic coatings using electrochemical methods is a relatively new technology that takes advantage of the large amount of literature available on metallic corrosion and electrodeposition [1-4]. There are several oxide film deposition technique, including physical deposition processes, such as vacuum deposition and sputtering using metal or oxide targets, and chemical deposition process, including spray coating, dip coating, and sol-gel techniques. In these coatings techniques, an amorphous film usually is deposited. As a consequence, a relatively high – temperature heat treatment is required to crystallize the film. The heat treatment, however, often causes peeling or cracking of the films because of reactions between substrate and film, shrinkage of the film, or thermal expansion mismatch. It also is difficult to deposit homogeneous films on substrates with complex shapes using these methods. Electrochemical coating techniques have several advantages over the more-conventional coating techniques. The thickness and morphology of the ceramic films can be controlled by the electrochemical parameters, and relatively uniform deposits can be obtained on complex shapes. Equally attractive is that the equipment is cheap, and the technique has the potential to synthesize crystalline films near room temperature in large-scale operations.

The interest in this electrochemical process is related to the control of the chemistry of the metal-electrolyte interface so that a desired reaction product be formed at the exposed surface. This is achieved by manipulating a combination of parameters, such as electrolyte composition, pH, temperature, applied voltage and current, and atmosphere. Electrochemical processes use the electrochemical potential of the material upon which the reaction product is be formed. Many types of

* Paper presented at Romanian Conference on Advanced Materials, Bucharest, Romania, October 23-25, 2000

ceramics are required in industry. For example, zirconia has been prepared in order to be used as a fiber coating material for promoting crack deflection and debonding at the fiber-matrix interface of alumina/alumina composites [5]. Also, zirconia films are used as thermal-barrier coatings, wear resistance coatings, diffusion barriers, oxygen sensors, and as underlayers for superconducting films [6]. Yttria stabilized zirconia coatings prepared by plasma spray or physical vapor deposition have been successfully used to protect Ni-based superalloy components from high-temperature turbine environment [7].

Cr_2O_3 is known for its high wear and corrosion resistance at high temperature, and is formed as a protective native oxide on high-temperature metallic superalloys [8]. It appears that the relatively low ductile-to-brittle transition temperature of these Cr_2O_3 coatings provides the ductility, which is necessary for erosion-resistance of turbine blade superalloys.

2. Experimental

Graphite bars of spectral purity, having diameter of 5 mm and high of 50 mm were used as the substrates. The electrolyte used was 0.1 M aqueous solution of $\text{Cr}(\text{NO}_3)_3 \cdot 9\text{H}_2\text{O}$ with an addition of 30 vol. % ethanol and an initial pH of 2.5. The 100 ml electrochemical cell contained a cathode substrate in the shape of a cylinder centered inside of a platinum wire spiral constituting the anode. A power supply, model MIM, supplied the necessary power, and the cell voltage and current were monitored with MAVO20. Cathodic polarization curves were estimated with a potentiostat model PAR 270, and the solution pH was measured with a SEIBOLO pH meter.

Deposits were formed at current densities from 5 to 90 mA/cm^2 and duration of 5 to 60 min., while the cell voltage, the pH, and the temperature of the solution were measured continuously. The experiments were performed without stirring. Our previous researches have shown that the stirring of solution determined a weak deposition [9]. The deposits were dried for 24 h in air at room temperature. Some of the specimens were sintered for 1h at 1100 °C in air. Coating weights were determined by weighing the specimens before and after deposition, using an electronic scale having an accuracy of ± 0.05 mg. Coating thickness was measured with the aid of a interferometric scanning microscope, model NV200, and an optical microscope calibrated in the direction perpendicular to the field of vision. The microstructures of the coatings were characterized before and after sintering, using the interferometric scanning microscope. The phase content was determined by X-ray diffraction with a diffractometer, model DRON3, operated at 30 kV and 20 mA, using monochromatized Cu $K\alpha$ radiation.

3. Results

3.1. Electrochemical characterization

Cathodic polarization curve with a saturated calomel electrode is shown in Fig. 1. Based on the typical shape expected for the polarization curve [10], it may be deconvoluted into two curves, each representing a different reaction. These reactions may be referred to the reduction of the dissolved oxygen and the nitrate, respectively. The third reaction, namely reduction of water, could not be detected due to the voltage limitation of the potentiostat (only 4V).

Coating weight as a function of current density and with constant coating duration (15 min.) is presented in Fig. 2. The coating weigh increases with current density to a maximum, reached at 25 mA/cm^2 . At current density below this maximum, the coating weight increases linearly with time, (Fig. 3), which points to an essentially constant deposition rate.

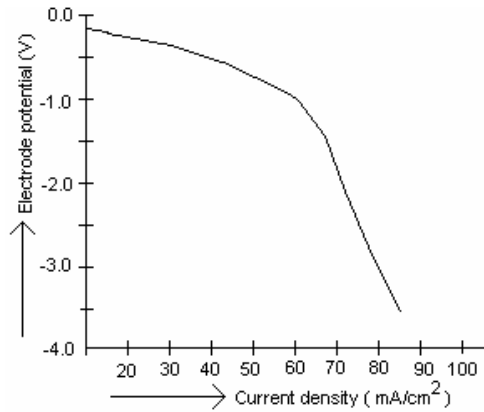


Fig. 1. Cathodic polarization curve.

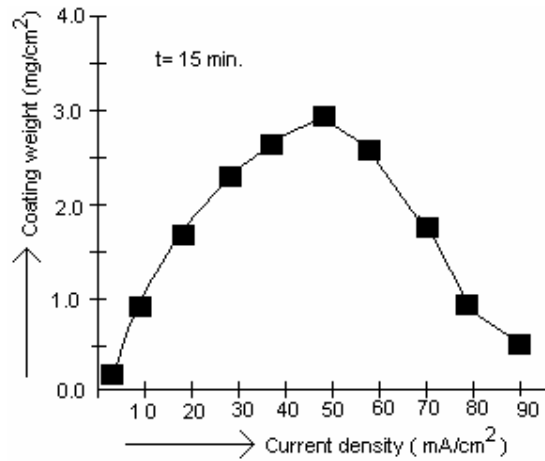


Fig. 2. Coating weight vs. current density.

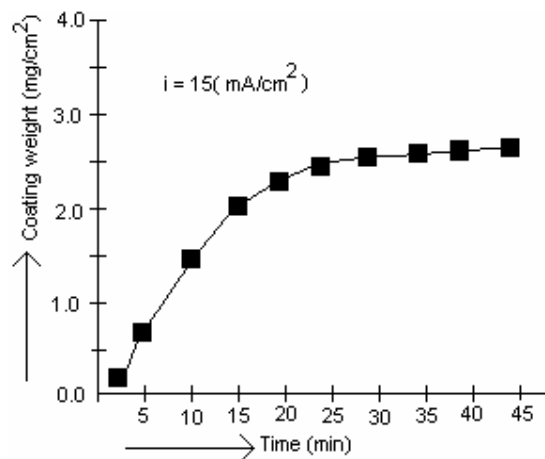


Fig. 3. Coating weight vs. electrodeposition time.

The decrease in the coating weights at higher current density was found to be accompanied by deposit spallation, due to the high evolution and release of bubbles at the cathode surfaces. The cell voltage increased with deposition time as can be seen in Fig. 4. At low current density this increase is linear, whereas at higher current density it was accelerated at short duration, but as the duration grew

up, the rate decreased. The pH level of the electrolyte at different current densities changed within the range of 2 to 3. Generally, above a current density of 20 mA/cm^2 , the pH of the solution increased during the first 2 min. of the deposition, and afterward tends to reach a maximum, which increases with current density. The change in the pH can be put in relation with the formation of hydroxyl ions and to the rate of their migration into the solution.

3.2. Microstructural characterization

Immediately following deposition, the chromia coatings are dark greenish and opaque. After drying the coatings present a lot of cracks. In the Fig. 5 an image of the coating morphology is shown. The homogeneity of the coating thickness and its morphology over the coated surfaces depend strongly upon the current density. At high current density, the rough of coating surfaces was characterized by presence of the concave cups localized at intersections of cracks. At lower current density, the magnitude of the drying microcracks in the coatings was similar to those at higher current density, though, initially, the microcracks were smaller. This aspect, which is associated with lower coating thickness, is characterized by microcracks having wavy surface, as compared with the straight cracks in thicker coatings.

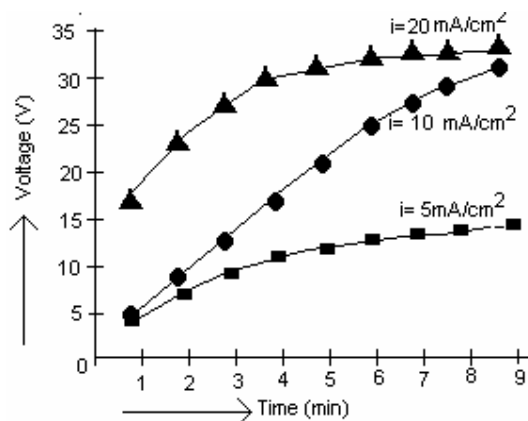


Fig. 4. Cell voltage vs. electrodeposition time.



Fig. 5. Optical image of chromia electrocoating obtained by scanning interferometric microscopy.

In Fig. 6 the X-ray diffraction spectrum of chromia coating is presented. It shows that this coating has a crystalline nature. A very sharp reflection of chromia with a corundum-type hexagonal structure was evidenced. The (116) reflection is very strong compared with those expected for the powder sample.

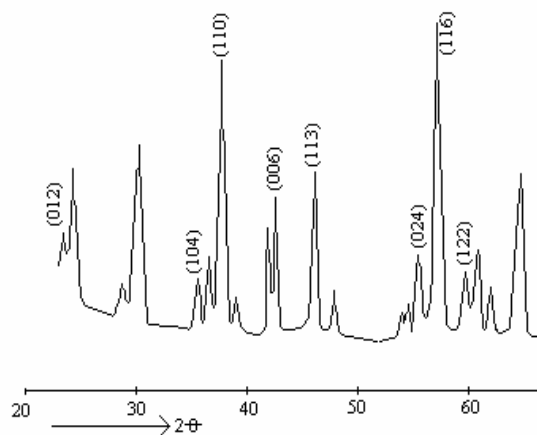


Fig. 6. X-ray diffraction pattern of electrodeposited chromia.

X-ray spectrum of electrocoating after sintering at $1100\text{ }^\circ\text{C}/1\text{h}$ is presented in Fig. 7 and no additional peaks were detected. A change in the relative intensities of Cr_2O_3 is observed. The spectrum demonstrates a finishing of the crystalline lattice of the electrocoating. No indications of the formation of reaction phase products were observed.

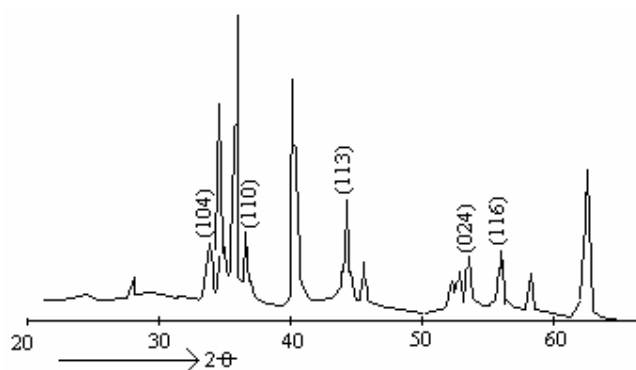


Fig. 7. X-ray diffraction pattern of electrodeposited chromia after sintering.

In Fig. 8 is presented the microstructure of Cr_2O_3 coating after sintering. One can see many droplets-like particles, which fill the previously empty microcrack gaps.

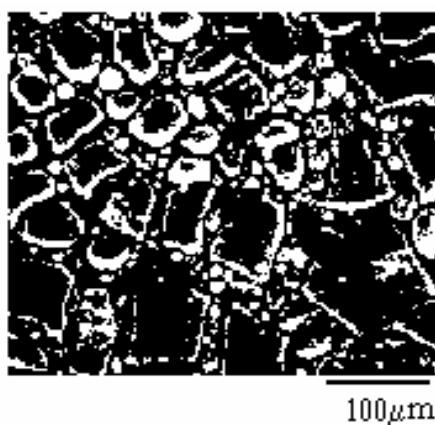


Fig. 8. Optical image of the sintered chromia electrocoating.

This microstructure is thought to be caused by an evaporation-condensation mechanism, which tends to densify the coating, by condensation of Cr_2O_3 at the microcrack spaces, thus creating a continuity between the coating islands. Simultaneously, the islands shrink in size, indicating the sintering of the green coatings. According to D. Blum, J. C. Guitel and P. Lofgren studies [11, 12], the structure of the Cr-O polyanions is basically that of linear chains of polyhedra with corner-to-corner bonds of either double, triple or quadruple-polyhedra. Condensation kinetics of the Cr-O polyhedra is considered to be relatively slow, which results in an open structure. Thus, the chromium oxide may be formed by migration of these polynuclear species toward the cathode. Further reconstruction of these polyhedra to the more closely packed structure may occur on the cathode surfaces and thus provide the nuclei for condensation mechanism, which tends to densify the coating by condensation of Cr_2O_3 crystals bonded to water molecules. Therefore, the chromia lattice contains water and hydroxyl ions, which are expected to distort it, according to Chaim et al. [13].

4. Conclusions

It is demonstrated that Cr_2O_3 can be prepared by an electrolytic method. It is shown that Cr_2O_3 coating can be controlled by means of the electrochemical parameters. On a graphite substrate, Cr_2O_3 coating is obtained, directly, in crystalline state. Water and hydroxyl ions disturb the crystalline lattice. After a sintering treatment, the crystalline lattice of Cr_2O_3 coating becomes more finished, the density of microcracks decreases and the porosity diminishes.

References

- [1] J. A. Switzer, *J. Am. Ceram. Soc. Bull.* **66**, 1521 (1987).
- [2] R. J. Phillips, M. J. Shane, J. A. Switzer, *J. Mater. Res.* **4**, 923 (1989).
- [3] I. Zithomirsky, L. Gal-Or, S. Klein, *J. Mater. Sci. Let.* **14**, 60 (1995).
- [4] W. Cho, M. Yashima, M. Kakihana, A. Kudo, T. Sakata, M. Yoshimura, *Appl. Phys. Lett.* **68**(1), 137 (1996).
- [5] P. Slezak, A. Wieckowski, *J. Electrochem. Soc.* **138**, 1038 (1991).
- [6] M. Pakala, H. Walls, R. Y. Lin, *J. Am. Ceram. Soc.* **80**(6), 1477 (1997).
- [7] R. Srinivasan, B. H. Davis, *J. Am. Ceram. Soc.* **75**(5), 1217 (1992).
- [8] R. Marvel, *Mater. Sci. Eng.*, **A120**(11), 13 (1989).
- [9] L. Gheorghies, Doctoral Thesis, University "Dunarea de Jos" of Galati, 1998.
- [10] C. Gheorghies, *J. Cryst. Growth* **213**, 112 (2000).
- [11] D. Blum, J. C. Guitel, *Acta Crystallogr.* **B36**, 135 (1980).
- [12] P. Lofgren, *Acta Crystallogr.* **B29**, 2141 (1973).
- [13] R. Chaim, I. Silberman, L. Gal-Or, *J. Am. Ceram. Soc.* **138**(7), 1942 (1991).